Sociedad Mexicana de Ingeniería Mecánica
Fecha de recepción: 05-02-2015
Fecha de aceptación: 25-05-2015

INGENIERÍA MECÁNICA
TECNOLOGÍA Y DESARROLLO
Vol. 5 No. 3 (2015) 339 - 345

Wear mechanisms experienced by an automotive grade Al-Si-Cu alloy under sliding conditions

Diego E. Lozano[1], Rafael. D. Mercado-Solís[1], A. Juarez-Hernandez[1]
M.A.L Hernández-Rodríguez[1], Nelson F. Garza-Montes-de-Oca[1*]
[1]Facultad de Ingeniería Mecánica y Eléctrica, Universidad Autónoma de Nuevo León
San Nicolás de los Garza, Nuevo León, México, 66450
* Corresponding author: nelson.garza@gmail.com

Resumen

Los mecanismos de desgaste que experimenta una aleación Al-Cu-Si fueron estudiados utilizando una maquina tribológica del tipo perno sobre disco bajo condiciones de lubricación y diferentes valores de carga normal. La microestructura de la aleación incluye una matriz de aluminio en la cual partículas ricas en silicio y compuestos intermetálicos se encuentran dispersos. Técnicas de microscopía óptica (MO) y electrónica (MEB) fueron utilizadas junto con análisis de espectroscopia rayos- X (ERX)) para caracterizar los diferentes rasgos de los procesos de desgaste que sufrió la aleación durante de las pruebas. El proceso de desgaste del material fue caracterizado por la fractura y posterior desprendimiento de las partículas primarias de silicio de la matriz de aluminio. Bajo esta condición de prueba, la rapidez de desgaste se ubica en el régimen de desgaste moderado. Las razones por las cuales diferentes mecanismos de desgaste ocurren así como las variaciones que experimenta el coeficiente de fricción durante las pruebas son discutidas en este trabajo.

Abstract

The wear mechanisms experienced by a cast hypereutectic Al-Si-Cu alloy were studied using a pin on disc tribometer, under lubricated sliding conditions at different normal loads. The microstructure of the alloy comprised primary silicon particles and intermetallic compounds dispersed in an aluminium matrix. Optical microscopy (OM) and scanning electron microscopy (SEM) coupled with energy dispersive X-rays (EDX) were used to characterize distinctive wear features after the tests. Wear of the alloy was characterized by fracture and spallation the intermetallic compounds and the primary silicon phases from the matrix. Under this test condition, the wear rate of the material corresponded to a mild wear regime. The reasons for the development of each wear mechanism and the variations of the friction coefficient of each test condition are discussed.

Palabras clave:
Aluminio, aleación automotriz, mecanismos de desgaste, MEB

Keywords:
Aluminium, automotive alloy, wear mechanisms, SEM

Introducción

Fuel consumption economy by means of body weight reduction represents a key objective for the automotive industry. Currently, the use of engine components manufactured from lightweight materials such as aluminium alloys has been considered, aiming to fully replace components made from iron alloys. However, since aluminium alloys exhibit low wear resistance, iron alloys remain as the material of choice for the manufacture of automotive components that are exposed to high friction and wear conditions, namely engine block cylinders and brake discs. The use of aluminium alloys for automotive applications depends entirely on the improvement of both, metallurgical processing and mechanical properties in order to develop products with enhanced tribological properties.

Even though many strategies like the application of hard coatings on the surface of aluminium alloys have been used to improve their wear resistance and mechanical properties[1], in many cases, the complex geometry of the components makes of these strategies a difficult process to conduct which is also expensive. To overcome these difficulties, efforts to increase the wear resistance of Al alloys have been developed from the metallurgical point of view this is; by adding different amounts of alloying elements[2]. From these, it is well known that silicon is added to Al alloys in different amounts to improve alloy hardness[2,3]. Unfortunately during normal operation conditions particularly in automotive applications, the temperature of the components tends to increase promoting a reduction in strength of Al-Si alloys[2,3], To overcome this problem elements like copper, magnesium, iron and strontium are also added to the alloys to promote microestructural stability by precipitation hardening[2,3].

Various investigations have been developed to understand the effect element additions on the wear resistance of aluminium alloys. For example, Wu and Zhang[4] studied the effect of Sn on the wear characteristics of hypereutectic alloys finding that the presence of this element increased its wear resistance and modified the wear mechanisms experienced under dry sliding conditions. In a different study, Goto *et al* [5] found that the wear and friction of graphite impregnated aluminium-silicon alloys is considerably low under lubricated conditions which makes this material suitable for automotive applications. Alternatively, Clarke and Sarkar[6] found a considerable increment on the wear resistance of aluminium alloys having silicon contents near to 12.6 %wt. For wear resistance applications in the automotive industry, hypereutectic aluminium alloys with silicon additions are commonly used[6-11]. It has been reported that the precipitation of primary silicon particles during the solidification, increases the load bearing capacity during sliding wear of these alloys[12,13]. Even tough the existence of large primary silicon particles in hypereutectic Al-Si alloys improves wear resistance; the presence of these phases in the alloy increases considerably the cost of the final product regarding tooling damage during the machining practices experienced on the components made from this material. In addition to the silicon content in the alloy, the size and distribution of the silicon particles in the matrix also play a key role in alloy design. It has been found that alloys containing small, better dispersed silicon particles resulted with superior wear resistance, compared with alloys that did not include them[14-18]. This phenomenon is normally caused by the addition of strontium, as an element that promotes the formation of numerous nuclei, favouring silicon modification and particle dispersion.

Another important aspect that promotes the use of aluminium alloys for tribological applications is the ability to form protective surface layers during relative motion and under contact conditions with other components. These layers comprise a mixture of material removed from the surface and oxides produced mainly by frictional heating, which combined, act as a hard protective tribofilm. Riahi and Alpas[17] found that by increasing the values of applied load and test speed, the thickness and hardness of the tribofilm formed on Al-Si alloys increased. Alternatively, Nicholls et al.[19] found that the metallic matrix in Al-Si alloys is removed during sliding contact together with primary silicon particles, action that favoured the formation of a composite tribofilm. Xia *et al*.[13] found that the nature and properties of the tribofilm formed during sliding contact depended mainly on the lubrication characteristics of the tribosystem.

In this investigation, the wear rate of a hypereutectic Al-13Si-4Cu alloy is assessed, aiming to determine the performance of the material and the dominant wear mechanisms when exposed to lubricated sliding conditions.

Experimental Procedure

The alloy for this study represents a development from an international manufacturer of automotive components and it was obtained from a low pressure sand casting process developed at 0.70 atm and 750°C. The molten metal was poured directly into the mould by pressurization of the furnace under a regime of low turbulence which was achieved by means of regulating both, the casting pressure and speed. Table 1 shows the chemical composition of the alloy.

Table 1. Chemical composition of the Al-Si-Cu alloy.

Alloying elements in %wt							
Al	Si	Cu	Fe	Ni	Sr	Mg	Mn
Balance	13.5	2.5	1.0	0.60	0.06	0.20	0.25

The molten metal was cast to the final shape of an engine block and after solidification and machining practices, it was subjected to a heat treatment route which comprised a solution treatment conducted for 5 hours at 495°C followed by rapid quenching to 90°C and finally and ageing treatment developed for 5 hours at 240°C.

The microstructure of the alloy resulting from the heat treatment practices included a hypereutectic Al-Si matrix, where small primary silicon needles and intermetallics such as Al-Ni-Cu, Al-Fe-Si-Mn-Cu and Al-Si-Sr were dispersed (Figure 1).

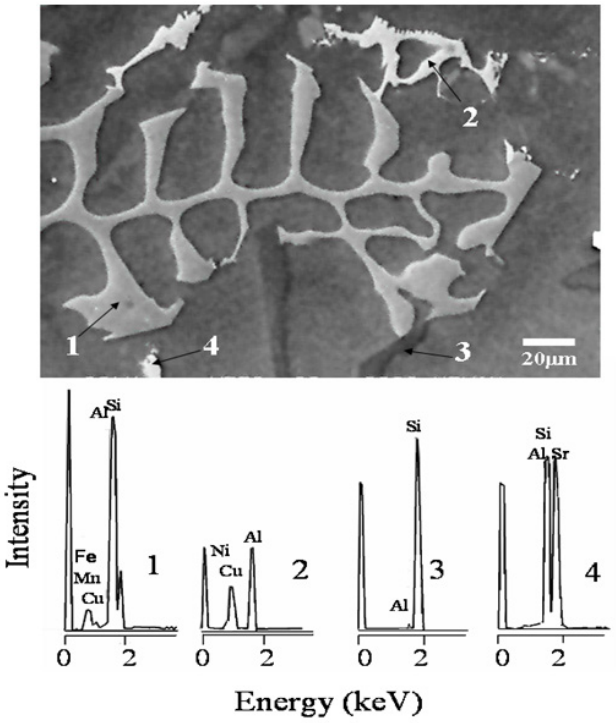

Figure 1. Intermetallic compounds present in the alloy.

The microhardness of the samples in as cast condition was determined using a Vickers indenter applying a load of 200 g for 15 seconds. The resultant average value of 113 ±8 HV which was obtained from measurements performed to 20 specimens. Alternatively, tensile tests were conducted to determine the Young's modulus of the alloy resulting in an average value of 92 ±3GPa.

For the tribological tests, AISI 52100 steel balls of 10 mm diameter and 924 HV hardness were used as counter part

according to the ASTM G99 standard. Alternatively, rings of 12 mm thickness, 115 mm external diameter and 100 mm internal diameter were machined directly from the heat treated alloy. Prior to the tests, the contact surface of the rings was prepared following standard metallographic procedures, using various grades of abrasive SiC paper and a final polishing stage with 1 µm Al_2O_3 powder to produce a mirror finish. Care was taken to repeat the same procedure for each specimen to have surface consistency. Roughness measurements were taken from the surface of each specimen using a stylus profilometer, resulting in an average Ra value of 0.12 ± 0.03 µm. Four measurements were taken from each test specimen on a sample length of 3 mm.

Lubricated test were developed using a pin on disc tribometer designed and constructed according to the ASTM G-99 specification (Figure 2).

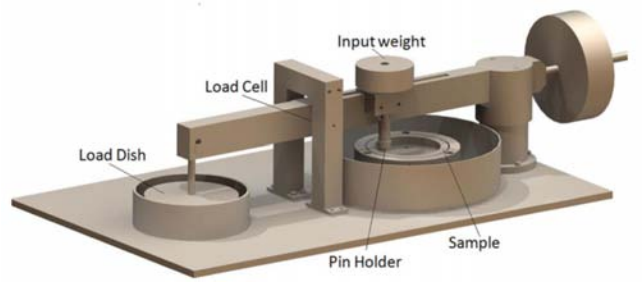

Figure 2. Pin-on-disc tribometer used for the wear tests.

The test rig comprises a lever arm mounted on two-axe pivots with ball bearings, allowing the arm to move frictionless. A load dish is attached at the end of the lever arm immersed in an oil container to act as a vibration absorber. On the opposite extreme of the arm, a counterweight is used to balance the load to zero. The normal load is applied directly on the pin holder, where the steel balls for the tests can be fixed. The holder for the ring-disc specimens comprises a 3-point levelling system which sets the ring perpendicular to the ball-pin holder allowing a maximum misalignment below 1º. The ring holder rotates in the horizontal plane. The friction force established between the ball and the ring drives the frictionless arm is measured by a load cell that registers the value of the lateral force established at the contact. A data acquisition system was used to record the values of friction force in order to calculate the friction coefficient using the equation:

$$\mu = \frac{F}{P} \tag{1}$$

where μ represents the friction coefficient, F is the average value of the friction force in N and P is the value of the applied normal load in N. Friction values were recorded at a rate of ten data points per second the average value with a ±0.006 standard deviation.

Before and after the tests, the specimens were cleaned by immersion in acetone in an ultrasonic bath. Once cleaned, the samples were weighed using an analytical balance with an accuracy of $\pm 1x10^{-4}$ mg.

Wear tests were conducted varying the applied load and sliding speed based on technical details and variables that were of interest for the process. The loads selected for this investigation were 30, 50 and 120 N and the sliding speeds 0.5, 1.0 and 1.5 m/s which correspond to angular speeds of 96, 198 and 285 rpm respectively. Experiments were conducted at different sliding distances up to 20 km repeating the tests in 2 specimens to obtain an average value. The experimental matrix for the test is shown in table 2.

Table 2. Experimental matrix for the development of the wear tests.

Speed (m/s)	Applied load (N)					
	30		50		120	
0.5	1	2	1	2	1	2
1.0	1	2	1	2	1	2
1.5	1	2	1	2	1	2

It is worth mentioning that the tests were conducted under lubricated conditions to emulate the condition found in an engine block. This was done by means of applying SAE 40 oil directly onto the surface of the sample at a constant speed and volume. During the tests, the lubricant was filtered before its return to the container to avoid contamination by foreign particles and wear debris.

The extent of wear experienced by the samples was measured by following the mass change of the specimens. Once the mass lost by the specimens was determined, the volumetric wear was calculated using the nominal density of the alloy (2.71 g/cm^3). The specific wear rate was then obtained using the equation:

$$\mathcal{W}^o = \frac{V}{SP} \tag{2}$$

where $\mathcal{W}^o$ is the specific wear rate in mm^3/N-m, V the volume of material removed in mm^3, S the sliding distance in m and P the normal load in N.

After the tests, the specimens were prepared for the inspection in a scanning electron microscope to determine the wear mechanisms. Analyses were conducted at various acceleration voltages and working distances using both, secondary (SE) and backscattered electron detectors (BSE). Energy dispersive analyses (EDX) were also performed on the specimens when it was required.

Results and Discussion

Figure 3 shows the effect of load and sliding speed on the behaviour of friction in lubricated condition.

Values of friction coefficient were observed between 0.06 and 0.13. It can be noticed that the friction coefficient decreased when the sliding speed increased. This can be explained based on the elastohydrodinamic lubrication theory, which proposes that the hydrodynamic pressure increases with the test speed of the system, reducing asperity contact and therefore the friction coefficient. Even though the third friction law points out that friction is independent of speed[21], this

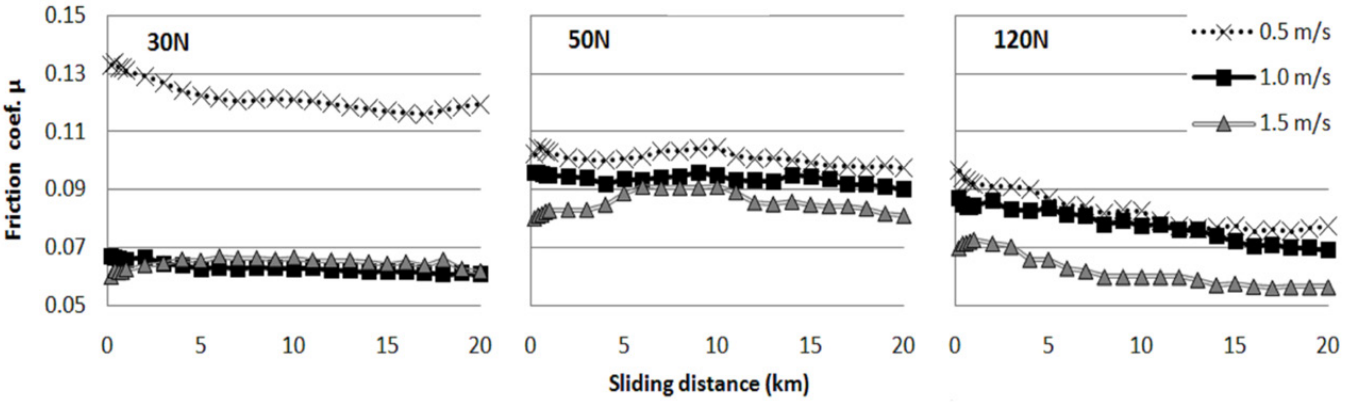

Figure 3. Behaviour of the friction coefficient as function of the applied load at various sliding speeds.

argument is commonly invalid. Commonly, the plot of the friction coefficient against the sliding speed gives a negative slope[22]. Bhushan[23] found that the effect of high normal loads combined with high sliding speeds produce elevated interfacial temperatures which reduce the shear strength of the asperities considerably and therefore, the value of the friction force at the interface, which agrees with the phenomenon here studied.

For all the tests where the 120 N normal load was applied, a progressive reduction in the value of the friction coefficient was observed as a function of the sliding distance which is consistent with the elasto-hydrodynamic lubrication theory[19].

From figure 3, it is also possible to appreciate that the value of the friction coefficient was reduced when the normal load increased. When increasing the value of the normal load, work hardening might be occurring at the surface of the alloy together with the formation of a mechanical mixed layer of a considerable hardness value, which increases the overall surface hardness of the alloy favouring a fall in the friction values. For the 120 N load tests where this phenomenon is more evident, it is possible that the shear stresses at the interface ball-ring were large enough to facilitate the removal of the Al-matrix, leaving the hard silicon particles exposed at the surface which may acted as load bearers that reduced friction as it is schematically presented in figure 4.

Figure 4. Schematic representation of the exposure of silicon particles as a consequence of Al-matrix removal during the wear test.

It is worth mentioning that friction was measured and recorded from the beginning of all the tests. Since both surfaces were considerably smooth and great amount of lubricant was supplied, is was not possible to distinguish the running-in period as an evident phenomenon.

The behaviour of the specific wear rate is shown in figure 5.

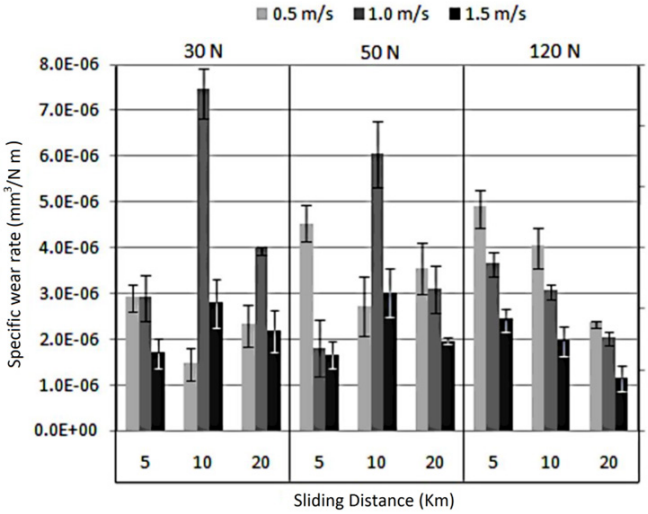

Figure 5. Specific wear rates measured for each test condition.

From this figure, it can be noticed that under this test conditions, the hypereutectic Al-Si-Cu alloy has a wear coefficient in the order of $1x10^{-6}$ which falls into the region of mild wear regime[22]. For the 30 and 50 N loads, it is not possible to distinguish a dominant wear mechanism from the values taken from the plots, but probably given the high values of applied load severe wear might be occuring. Although friction for 30N load was higher at 0.5m/s, the maximum specific wear rate observed was at the 30 N and 1.0 m/s test condition. A similar behaviour was observed for the tests developed at the 50 N load, which experienced the highest wear rate with the 1.0 m/s speed at approximately 10 km of sliding distance. For the highest load studied (120N), the specific wear rate was considerably higher up to a distance of 5 km, if this is compared with the specific wear rate obtained at the lower loads for all the test speeds. There is also a trend of the wear rate to decrease with an increase of the sliding distance; this is, 50% of wear occurred during the first 5 km, 30-40 % of wear occurred from 5 to 10 km, and the remaining 10-20% from 10 km to 20 km. This trend agrees well with the friction behaviour of the specimens tested under the 120 N load, and can be explained in a similar manner as in the case of

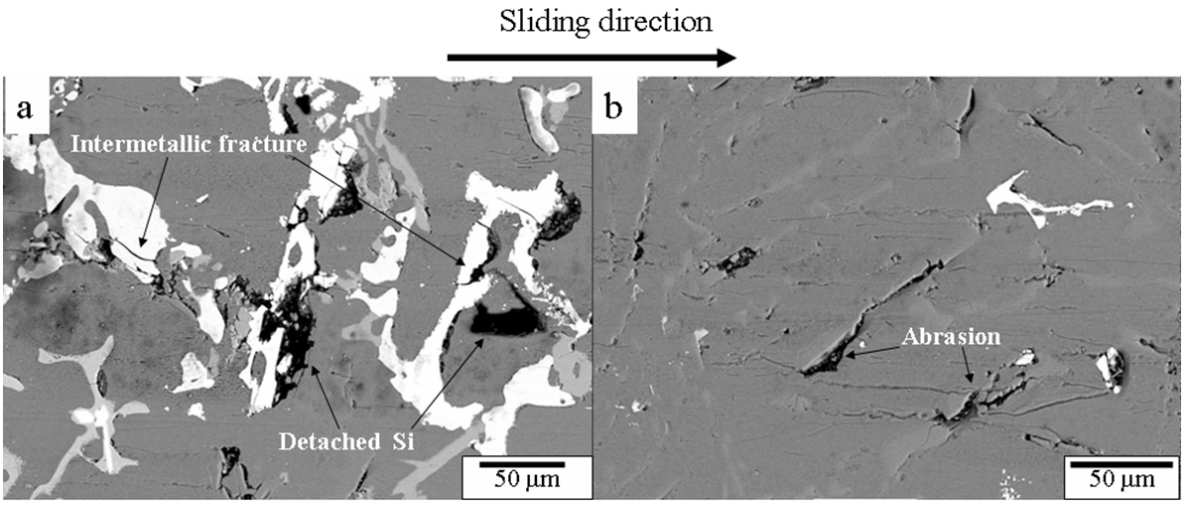

Figure 6. a) Backscattered electron micrographs showing the worn surface by intermetallic fracture obtained at 30 N load, 1 m/s and 20 km of sliding distance, b) Plastic deformation of the surface is clearly evident.

friction i.e. the formation of a tribofilm on the surface of the alloy also accounted to reduce wear by protecting the surface against the damage exerted by both, the asperities of the ball and the material removed from the alloy during the test.

Figure 6 shows SEM micrographs of the worn surfaces obtained from the tests conducted under the 30 N load.

It is possible to observe that the Al-Fe-Cu intermetallics were fractured preferentially (Figure 6a); revealing also the sites where silicon particles were present in the matrix prior their removal. In addition, abrasion patterns were also appreciated (Figure 6b) on the surface of the specimens along the sliding direction produced by work hardened aluminium and silicon particles that where removed during the tests.

Figure 7 a and b respectively show backscattered electron micrographs taken from the surface of the specimens tested at 50 N normal load.

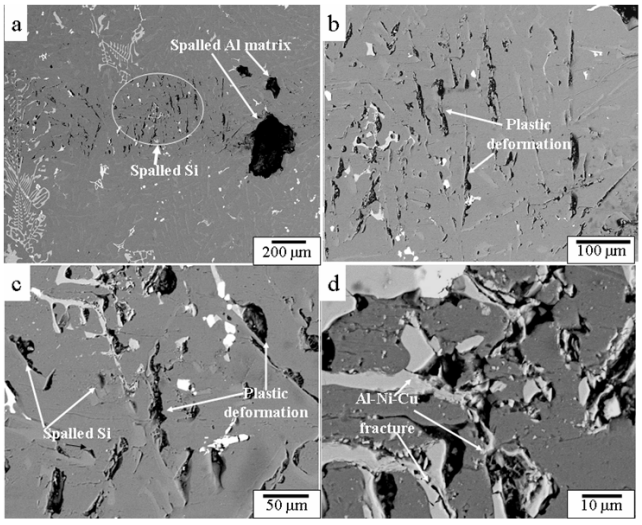

Figure 7. a) Backscattered electron micrographs showing the worn surface obtained at 50 N load, 1 m/s and 20 km of sliding distance, spallation of Al and Si particles, b) Plastic deformation in the Al matrix, c) and d), plastic deformation and intermetallic fracture.

From these micrographs, it is observed that primary Si particles and fragments from the matrix of considerable size were removed. Patterns of plastic deformation in the matrix are also evident. The spallation of microstructural components and the fracture of Si particles of can be better appreciated in figure 7 c and d respectively. The fracture of the intermetallic compounds, favoured the formation of particles of small size which were embedded into the surface as the test progressed, increasing the plastic deformation of the matrix by abrasion. Al-Ni-Cu intermetallics presented minimum damage under this condition expressed as the formation of fractures of small size.

Figure 8 shows backscattered electron micrographs of typical surface damage found in the specimens after the tests conducted at 120N.

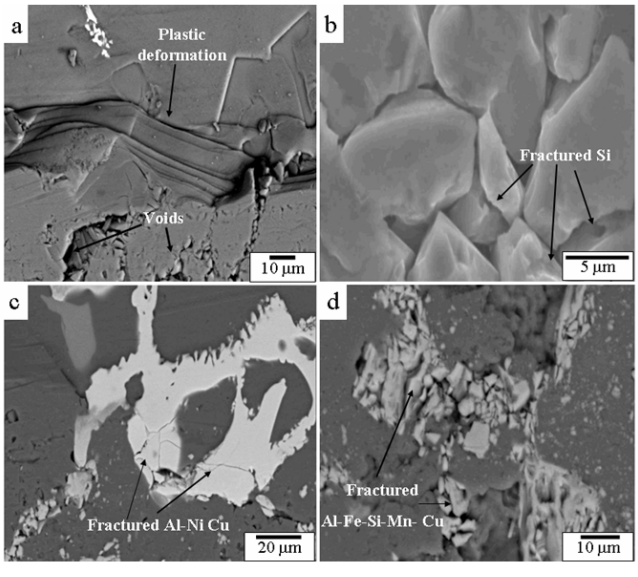

Figure 8. Backscattered electron micrographs showing the worn surface obtained at 120 N load, 1 m/s and 20 km of sliding distance. Severe plastic deformation of the Al matrix (a). Fracture of silicon particles (b). Fracture of Al-Ni-Cu intermetallics (c). Fracture of Al-Fe-Si-Mn-Cu intermetallics (d).

In figure 8a, severe plastic deformation of the metallic matrix can be appreciated. This mechanism was as representative feature found on the surface of the material under this test condition. For this load value, test configuration and alloy, a high value of contact pressure of 16 GPa existed according to contact mechanics, which is maybe the reason for the severe damage experienced by the material. From this micrograph (Figure 8a), it also possible to appreciate the formation of voids: these sites were formed as result of the spallation of silicon particles and intermetallics from the matrix. Figure 8b shows a greater detail image where it is possible to appreciate that the silicon particles were fractured, a mechanism that favoured the formation of surface voids.

As it was previously mentioned, the matrix of the test specimens experienced severe plastic deformation and wear debris was mechanically mixed into the alloy increasing its hardness. Figure 8 c and d present Al-Fe-Si-Mn-Cu and Al-Ni-Cu intermetallic compounds showing severe fracture under this test condition, a mechanism that definitely accounted for the generation of abrasive wear debris and therefore, to increase wear in the alloy.

It is worth mentioning that subsurface damage was only observed for the specimens tested 120 N load. Figure 9a shows a cross section of the material which presents severe subsurface damage, expressed as the fracture of the intermetallic compounds and plastic deformation of the Al matrix.

From this figure, it is also possible to identify that a film covered the alloy surface. This film was exclusive of this test condition, formed probably by a mixture of fragments of both, the metallic matrix and the intermetallic compounds, resulting in a composite oxide layer. Undoubtedly, the formation mechanism, properties and exact composition of this layer deserves a more detailed investigation. Figure 9b gives a low magnification micrograph where the extent of the subsurface cracking phenomenon, the tribofilm and the plastic deformation of the alloy can be better appreciated. Even tough subsurface damage was clearly observed under this condition together with severe plastic deformation; the wear rate of the alloy decreased progressively when increasing the sliding distance and the sliding speed. Higher values of load and speed favoured the removal of material from the surface and therefore the formation of the tribofilm which at some point, acted as a protective layer under this test condition.

Conclusions

The wear behaviour of a hypereutectic Al-Si-Cu alloy against steel was studied. The alloy exhibited mild wear under lubricated conditions. The results suggest a better tribological performance of the alloys at higher loads, where friction and specific wear rate decreased with the sliding distance probably due to the formation of a protective tribofilm.

At higher normal loads, the Al-matrix is removed from surface after contact with the hard asperities of the steel, leaving Si particles as protruding isles at the contact surface. These silicon particles act as load bearing and energy absorbers which reduce friction and consequently the wear rate.

At higher normal loads, work hardening also occurs at the surface by a mechanism that includes the embedment of wear debris into the surface, producing a hard composite coating. The mechanical properties, chemical composition and protection mechanisms of this coating should be studied with fine detail.

Properly dispersed needle-like silicon particles enhance the wear resistance of the alloy since these do not experience considerable removal from the alloy matrix reducing the possibility of a three body wear scenario which could increase wear of the alloy.

Acknowledgements

The authors would like to thank The National Council for Science and Technology in Mexico (CONACYT), The Program for Lecturer Development (PROMEP), and Universi-

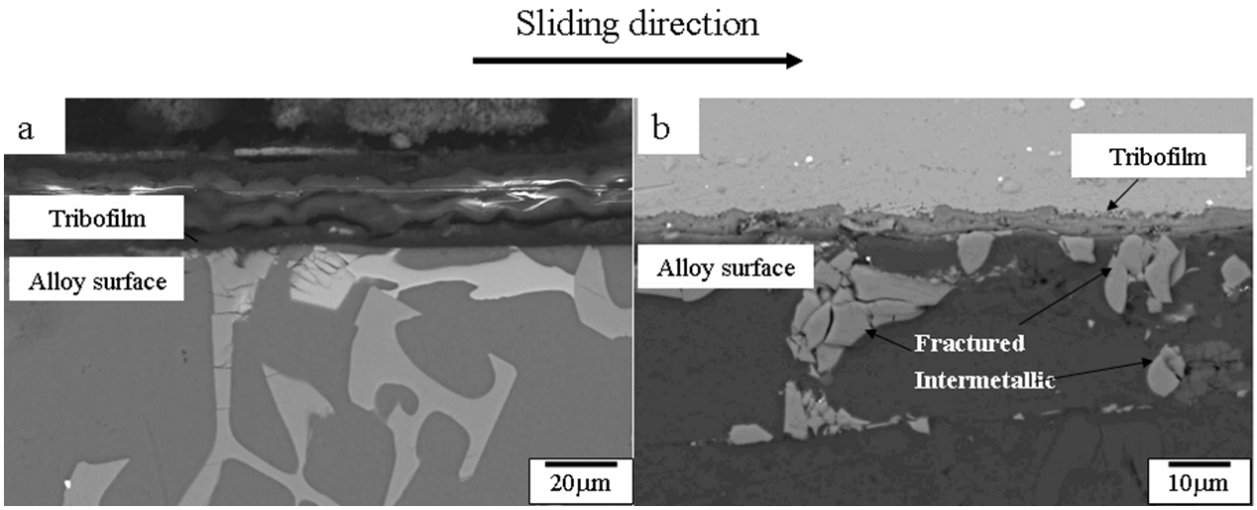

Figure 9. Cross sections of the material tested at 120 N, 20km and 1 m/s. Tribofilm formation and fracture of the intermetallic compounds (a). Severe plastic deformation of the aluminium matrix and fracture of the intermetallic compounds (b).

dad Autónoma de Nuevo León (UANL) for the support provided to develop this work.

References

[1] M. Treviño, N.F. Garza-Montes-de-Oca, A. Pérez, M.A.L., Hernández-Rodríguez, A. Juárez, R. Colás, Wear of an aluminium alloy coated by plasma electrolytic oxidation. Surface and Coatings Technology, 206 (2012) 2213-2219.

[2] J.A. Lee, Cast Aluminium alloy for high temperature applications, Automotive alloys The 132nd TMS Annual Meeting & Exhibition (2003)

[3] Matsuura, K., Ohmi, T., Kudoh, M., Takahashi, H., Kinoshita, H., & Suzuki, K. (2004). Dispersion strengthening in a hypereutectic Al-Si alloy prepared by extrusion of rapidly solidified powder. Metallurgical and Materials Transactions A, 35(1), 333-339.

[4] X.F. Wu and G.A. Zhang, Influence of Sn content on the microstructure and dry sliding wear behaviour of hypereutectic Al-20Si alloy, J. Mat Sci. 46 (2011) 7319-7327.

[5] H. Goto, C.V. Siciu and T. Inokuchi, Friction and wear properties of aluminum-silicon alloy impregnated graphite composite (ALGR-MMC) under lubricated sliding conditions, Tribol. Trans. 52 (2009) 331-345.

[6] J. Clarke and A.D. Sarkar, Wear characterization of as cast binary aluminum-silicon alloys, Wear 54 (1979) 7-16.

[7] T. Konishi, E.E. Klaus and J.L. Duda, Wear characteristics of aluminum-silicon alloy under lubricated sliding conditions, Tribol. Trans. 39 (1996) 811-818.

[8] M. Elmadagli and A.T. Alpas, A Parametric Study of the Relationship between Microstructure and Wear Resistance of Al-Si Alloys, Wear 262 (2007) 79-92.

[9] D.K. Dwivedi, Sliding temperature and wear behaviour of cast Al-Si-Mg alloy, Mater. Sci. Eng. A. 382 (2004) 328-334.

[10] M. Dienwiebel, K. Pöhlmann and M. Sherge, Origins of the wear resistance of AlSi cylinder bore surfaces studies by surface analytical tools, Tribol. Int. 40 (2007) 1597-1602.

[11] D.K. Dwivedi, Wear behaviour of cast hypereutectic aluminium silicon alloys, Mater. Des. 27 (2006) 610-616.

[12] M. Warmuzek, ASM International (2004) 1-9

[13] X. Xia, A. Morina, A. Neville, M. Priest, R. Roshan, C.P. Warrens and M.J. Payne, Friction modelling of tribofilm performance in a bench tribometer for automotive engine lubricants, J. Eng. Tribol. 222 (2008) 305-314.

[14] R.J. Donahue, W.G. Hesterberg and T.M. Cleary, Hypereutectic aluminum-silicon alloy having refined primary silicon and a modified eutectic, United States (1993) Patent 5234514

[15] G.F. Bolling and J. Cisse, Aluminum silicon alloys, United States (1975) Patent 3895941.

[16] K. Tsushima, M. Sayashi, M. Shioda, H. Kambe, S. Kitaoka, A. Hashimoto and H. Kattoh, SAE (1999) 01-0350 .

[17] A.R. Riahi and A.T. Alpas, The role of tribo-layers on the sliding wear behavior of graphitic aluminum matrix composites, Wear 251 (2001) 1396-1407.

[18] D.E. Lozano, R.D. Mercado-Solis and A.J. Perez, Tribological behaviour of cast hypereutectic Al–Si–Cu alloy subjected to sliding wear, Wear 297 (2009) 545-549.

[19] M.A. Nicholls, P.R. Norton, G.M. Bancroft and M. Kasrai, Chemical and mechanical analysis of tribofilms formed from fully formulated oils, Wear 257 (2004) 311-328.

[20] I.M. Hutchings, “Friction and wear of engineering materials”, Ed. Butterworth-Heinemann, Oxford, U.K, 1992.

[21] C.A. Coulomb, Mem. Math. Phys. X. (1785) 61-342.

[22] [22] E. Rabinowicz, Friction and wear of materials, Ed. Wiley, London, U.K, 1995

[23] B. Bhushan, Principles and applications of tribology, Ed. John Wiley & Sons, New York, USA, 1999.